JACS
JOURNAL OF THE AMERICAN CHEMICAL SOCIETY
Communication
pubs.acs.org/JACS

Covalent Immobilization of Oriented Photosystem II on a Nanostructured Electrode for Solar Water Oxidation

Masaru Kato,[†] Tanai Cardona,[‡] A. William Rutherford,[‡] and Erwin Reisner*,[†]

[†]Department of Chemistry, University of Cambridge, Lensfield Road, Cambridge CB2 1EW, U.K.
[‡]Department of Life Sciences, Imperial College London, London SW7 2AZ, U.K.

Supporting Information

ABSTRACT: Photosystem II (PSII) offers a biological and sustainable route of photochemical water oxidation to O_2 and can provide protons and electrons for the generation of solar fuels, such as H_2. We present a rational strategy to electrostatically improve the orientation of PSII from a thermophilic cyanobacterium, *Thermosynechococcus elongatus*, on a nanostructured indium tin oxide (ITO) electrode and to covalently immobilize PSII on the electrode. The ITO electrode was modified with a self-assembled monolayer (SAM) of phosphonic acid ITO linkers with a dangling carboxylate moiety. The negatively charged carboxylate attracts the positive dipole on the electron acceptor side of PSII via Coulomb interactions. Covalent attachment of PSII in its electrostatically improved orientation to the SAM-modified ITO electrode was accomplished via an amide bond to further enhance red-light-driven, direct electron transfer and stability of the PSII hybrid photoelectrode.

Solar light driven splitting of water into its elements is a sustainable route to generate hydrogen-based fuels.[1] A major challenge in water splitting is the thermodynamically uphill reaction of water oxidation to O_2, which involves a four-electron and four-proton transfer process. Photosystem II (PSII) is the natural water oxidation enzyme managing light absorption, charge separation, and the extraction of electrons and protons through the oxidation of water in a pH neutral aqueous solution.[2] PSII operates at a high rate; it oxidizes ~100 water molecules per second during full sunlight irradiation with an upper turnover number estimated to be $\sim 1 \times 10^6$ within the lifetime of the [Mn_4Ca] water oxidation catalyst.[3] PSII therefore serves as the unchallenged benchmark and an inspiration in photocatalytic water oxidation.[4]

Protein film photoelectrochemistry (PF-PEC), the photochemical analogue to protein film electrochemistry,[5] is currently in its infancy as a probe to study the function of photosynthetic enzymes, such as photosystem I and PSII.[6] PF-PEC is thereby a promising technique to study the photocatalytic rates and performance of photosynthetic enzymes under different conditions. We have recently reported on direct electron transfer (DET) from PSII to a mesoporous indium tin oxide (*meso*ITO) electrode.[6c] PSII was adsorbed to the bare ITO surface in a random orientation and the three-dimensional and transparent *meso*ITO electrode allowed for good electrical conductivity and high PSII loading.[6c] Several redox enzymes with biotechnological relevance, such as hydrogenases[7] and laccases,[8] were previously immobilized on electrodes in a controlled orientation to improve DET and the electrostability of the enzyme in protein film electrochemistry. Compared to these enzymes, the controlled immobilization of PSII on electrodes is not straightforward: PSII is photoactive and relatively huge (a molecular weight of ~700 kDa and a size of $10.5 \times 20.5 \times 11.0$ nm^3 for cyanobacterial PSII dimers),[2a,b] and its electron donation sites to electrodes are placed on one region at the stromal side of PSII (Figure 1).

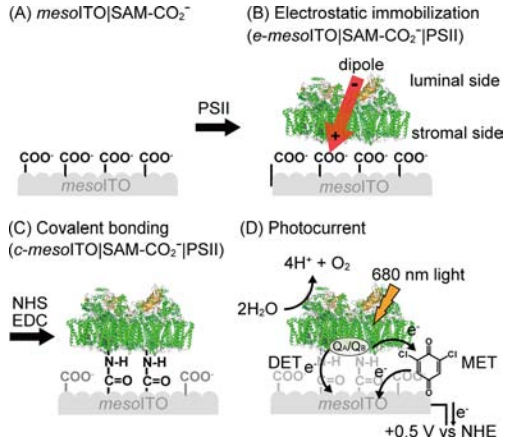

Figure 1. Schematic representation for the assembly of (A) *meso*ITO|SAM-CO_2^-, (B) electrostatic immobilization of PSII (*e-meso*ITO|SAM-CO_2^-|PSII), and (C) covalent bonding (*c-meso*ITO|SAM-CO_2^-|PSII). (D) Red-light-driven DET and 2,6-dichloro-1,4-benzoquinone MET resulting in photocurrents with *c-meso*ITO|SAM-CO_2^-|PSII.

We report on a rational protocol to improve the orientation of a cyanobacterial PSII on a self-assembled monolayer (SAM)-functionalized *meso*ITO electrode resulting in improved interfacial electronic communication between ITO and PSII. Covalent immobilization of oriented PSII to the electrode surface further improved DET and the stability of the enzyme (Figure 1).

*Meso*ITO electrodes with a geometrical surface area of 0.25 cm^2 were synthesized by annealing a paste of ITO nanoparticles (<50 nm diameter, 20 wt% in acetic acid/EtOH) on ITO-coated glass slides at 450 °C. The *meso*ITO electrodes (sheet

Received: May 10, 2013
Published: July 5, 2013

dx.doi.org/10.1021/ja404699h | J. Am. Chem. Soc. 2013, 135, 10610−10613

resistance of ~8 kΩ sq^{-1}, sheet thickness of ~3 μm)[6c,9] were modified with different phosphonic acid-linked SAMs (*meso*-ITO|SAMs). Phosphonic acids are commonly used to modify inorganic oxide surfaces including ITO with high surface coverage and stability in aqueous solutions.[9,10] The phosphonic acid compounds (1 mM, Chart 1) were self-assembled on

Chart 1. Compounds Used for SAMs on *meso*ITO

SAM	R	*n*	Abbreviation
H_2O_3P–(CH$_2$)$_n$–R	CO_2H	2	SAM-$C_2CO_2^-$
	NH_2	2	SAM-$C_2NH_3^+$
	CO_2H	5	SAM-$C_5CO_2^-$
	CO_2H	15	SAM-$C_{15}CO_2^-$

*meso*ITO from an ethanolic solution containing NEt_3 (2 mM) for 24 h, followed by heating at 140 °C under N_2 for 24 h and rinsing with NEt_3 (5% *v*/*v*) in EtOH (see Supporting Information, SI). The dangling carboxylic acid and amine functionality resulted in negatively and positively charged SAMs under pH neutral conditions, respectively.

Protein film electrochemistry requires only a small amount of enzyme sample to give good quality electrochemical data.[5] We minimized the amount of sample required in this study, and 2 μL of a PSII solution (0.067 mg Chlorophyll *a* mL^{-1}, 1.1 pmol PSII) were drop-cast on *meso*ITO|SAM. After 30 min in the dark, the electrode was rinsed with a buffered solution (10 mM MES, pH 6) to remove weakly bound PSII from the surface before immersing the electrode into the electrolyte buffer. This procedure allowed for electrostatic immobilization of PSII on the charged *meso*ITO|SAM surface (*e-meso*ITO|SAM|PSII). The optical transparency of ITO[9,10c] allowed us to record electronic absorption spectra in transmission mode of *e-meso*ITO|SAM|PSII, which showed the expected features of PSII on ITO with an absorbance maximum at 675 nm (see Figure S1).[11] The amount of PSII on the electrode was quantified by recording UV−vis absorption spectra of chlorophyll *a* in PSII in solution after desorption of the enzyme from ITO (see SI) for *meso*ITO|PSII without SAM (0.27 ± 0.07 pmol), *e-meso*ITO|SAM-$C_2NH_3^+$|PSII (0.35 ± 0.05 pmol), and *e-meso*ITO|SAM-$C_2CO_2^-$|PSII (0.39 ± 0.03 pmol, Table 1).

Photocurrent responses of *meso*ITO|PSII (in the absence of SAM, unmodified *meso*ITO), *e-meso*ITO|SAM-$C_2CO_2^-$|PSII,

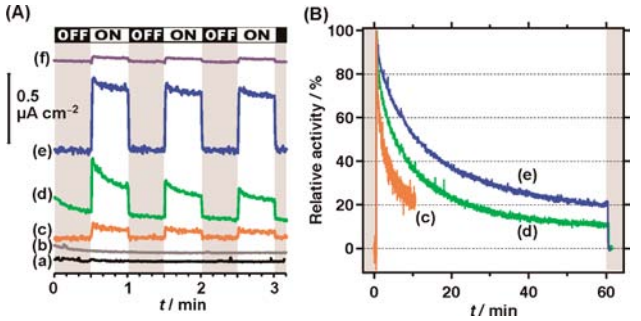

Figure 2. (A) Photocurrent responses under red-light irradiation (679 nm, 10 mW cm^{-2}) at +0.5 V vs NHE at 25 °C of (a) *meso*ITO|SAM-$C_2CO_2^-$, (b) *meso*ITO|SAM-$C_2CO_2^-$ treated with EDC and NHS, (c) *meso*ITO|PSII without SAM, (d) *e-meso*ITO|SAM-$C_2CO_2^-$|PSII, (e) *c-meso*ITO|SAM-$C_2CO_2^-$|PSII, and (f) *c-meso*ITO|SAM-$C_2CO_2^-$|PSII without the [Mn_4Ca] water oxidation catalyst (covalently linked Mn-depleted PSII). A buffered electrolyte solution at pH 6.5 was used, and no diffusional redox electron mediator was present. A checkered bar shows a light on and off cycle. (B) Photocurrent stability of electrodes (c−e) under continuous red-light irradiation at +0.5 V vs NHE.

and *e-meso*ITO|SAM-$C_2NH_3^+$|PSII were recorded under red-light irradiation (679 nm, 10 mW cm^{-2}) at pH 6.5 at 25 °C (Figure 2). DET occurred from PSII to ITO in all cases, but the carboxylic acid SAM resulted in the highest photocurrent response (0.28 ± 0.07 μA cm^{-2}, Table 1). A 3-fold increase in initial DET photocurrent was observed for *e-meso*ITO|SAM-$C_2CO_2^-$|PSII compared to *meso*ITO|PSII without SAM and *e-meso*ITO|SAM-$C_2NH_3^+$|PSII. No significant difference was observed in photocurrent responses of mediated electron transfer (MET) between *meso*ITO|PSII without SAM, *e-meso*ITO|SAM-$C_2CO_2^-$|PSII, and *e-meso*ITO|SAM-$C_2NH_3^+$|PSII (0.9−1.4 μA cm^{-2}), where a diffusional redox mediator, 2,6-dichloro-1,4-benzoquinone, was used. This observation suggests that the negatively charged *meso*ITO|SAM-$C_2CO_2^-$ surface resulted in improved orientation of PSII on ITO and, consequently, enhanced interfacial electronic communication between PSII and ITO. No photocurrent was observed in the absence of PSII for *meso*ITO|SAM-$C_2CO_2^-$. PSII in the absence of the [Mn_4Ca] water oxidation catalyst (Mn-depleted PSII)[11] on *meso*ITO|SAM-$C_2CO_2^-$ resulted in only a minor photocurrent (<0.02 μA cm^{-2}), demonstrating that the photocurrent responses resulted from water oxidation.

Table 1. Summary of DET and MET photocurrent responses (*j*, μA cm^{-2}), amounts of PSII immobilized on *meso*ITO (pmol) and turnover frequencies (TOFs, mol O_2 (mol PSII)$^{-1}$ s^{-1}) of *e-* and *c-meso*ITO|SAM|PSII electrodes

	j, μA cm^{-2}[a]			TOF, mol O_2 (mol PSII)$^{-1}$ s^{-1}[c]	
	DET	MET	PSII, pmol[b]	DET	MET
*e-meso*ITO|SAM|PSII					
SAM-$C_2CO_2^-$	0.28 ± 0.07	1.4 ± 0.6	0.39 ± 0.03	0.33 ± 0.07	1.4 ± 0.6
SAM-$C_2NH_3^+$	0.09 ± 0.02	1.1 ± 0.1	0.35 ± 0.05	0.09 ± 0.02	1.5 ± 0.2
unmodified (no SAM)	0.08 ± 0.01	0.9 ± 0.1	0.27 ± 0.07	0.18 ± 0.02	1.4 ± 0.2
*c-meso*ITO|SAM|PSII					
SAM-$C_2CO_2^-$	0.43 ± 0.03	4.5 ± 0.2	0.50 ± 0.06	0.61 ± 0.12	4.6 ± 0.6
SAM-$C_5CO_2^-$	0.25 ± 0.03	3.4 ± 0.8	0.38 ± 0.02	0.37 ± 0.10	5.7 ± 1.4
SAM-$C_{15}CO_2^-$	<0.02[d]	2.6 ± 0.6	0.36 ± 0.06	<0.03[d]	4.6 ± 0.8

[a]Initial photocurrents measured with a bias potential of +0.5 V vs NHE in an aqueous electrolyte buffer solution (pH 6.5) under red-light illumination (679 nm, 10 mW cm^{-1}) at 25 °C. Photocurrent responses for MET were recorded in the presence of 2,6-dichloro-1,4-benzoquinone (1 mM) in the electrolyte solution. [b]Amount of PSII on a *meso*ITO electrode (0.25 cm^{-2} geometrical surface area). [c]TOFs were calculated based on photocurrent densities obtained during 30 s red-light illumination with four electrons per O_2. [d]No photocurrent detected.

dx.doi.org/10.1021/ja404699h | J. Am. Chem. Soc. 2013, 135, 10610−10613

Photoinduced DET from PSII to an electrode can only take place through one region at the stromal side of PSII (Figure 1), and the results with electrostatically immobilized PSII can be explained by taking into consideration the dipole moment of PSII. Its positive dipole vector is located on the stromal side of the thylakoid membrane, where the potential electron donor sites, in particular the quinones Q_A and Q_B, are located (Figure 1). Analysis of the crystal structures of PSII from *Thermosynechococcus elongatus*[12] and *Thermosynechococcus vulcanus*[2b] showed strong dipole moments of 17357 and 16513 D, respectively, from the luminal surface to the stromal surface (Figure S2).[13] PSII can therefore orient itself on negatively charged surfaces in a favorable orientation during the adsorption process, which is in agreement with the 3-fold enhanced interfacial DET using the *meso*ITO|SAM-$C_2CO_2^-$ electrode.

Subsequently, we investigated the effect of covalent immobilization of oriented PSII on carboxylate-functionalized *meso*ITO. Treatment of *e-meso*ITO|SAM-$C_2CO_2^-$|PSII with 6 μL of the coupling agents EDC (36 mM) and NHS (17 mM) in MES solution (10 mM, pH 6) for 2 h yielded covalently amide-bonded PSII electrodes (*c-meso*ITO|SAM|PSII, Figure 1). The covalent bonding method led to the immobilization of 0.50 ± 0.06 pmol of PSII on *c-meso*ITO|SAM-$C_2CO_2^-$|PSII.

The covalently bonded PSII shows further enhanced photocurrents (0.43 ± 0.03 μA cm^{-2}) compared to electrostatically adsorbed PSII on *meso*ITO (Table 1). The covalent immobilization of PSII on ITO also resulted in an increased stability of the photocurrent responses compared to electrostatically adsorbed PSII (Figure 2B). *C-meso*ITO|SAM-$C_2CO_2^-$|PSII showed a significantly slower photocurrent decay (half-life time ~12 min) compared to the electrostatically bonded PSII on the SAM-functionalized and SAM-free *meso*ITO electrodes (both have half-life times of <5 min) during continuous red-light illumination. About 20% and 10% of the initial photocurrent remained after 1 h of continuous light illumination for covalently and electrostatically bonded PSII, respectively (Figure 2B). A positively charged ITO surface (isoelectric point of ITO: 7.4)[14] and a positive bias potential (+0.5 V vs NHE) result presumably in electrostatic repulsion with the positive dipole region of stromal PSII. Thus, the covalent bonding showed increased stability of the photocurrent of *c-meso*ITO|SAM-$C_2CO_2^-$|PSII.

To study the electrostatic preorientation in more detail, we prepared *c-meso*ITO|SAM-$C_2CO_2^-$|PSII by a different method. First, *meso*ITO|SAM-$C_2CO_2^-$ was activated with EDC and NHS (thereby removing the negative charge of the functionalized *meso*ITO for Coulomb attraction with the PSII stromal side), followed by addition of PSII on the neutral, NHS-activated *meso*ITO|SAM-$C_2CO_2^-$. The resulting electrode gave a DET photocurrent response of only 0.22 ± 0.01 μA cm^{-2}, supporting that the electrostatic orientation of PSII on *meso*ITO|SAM-$C_2CO_2^-$ prior EDC and NHS treatment puts PSII in favorable orientations for interfacial DET.

Photocurrent responses of *c-meso*ITO|SAM-$C_2CO_2^-$|PSII were also recorded at different bias potentials in the range between +0.25 and +0.70 V vs NHE (Figure S3). A minimal bias potential of +0.30 V vs NHE was required to observe photocurrent responses for *c-meso*ITO|SAM-$C_2CO_2^-$|PSII. The photocurrent response of *c-meso*ITO|SAM-$C_2CO_2^-$|PSII also reflects the intrinsic activity of PSII with the highest activity at pH 6.5.[15] Decreased DET photocurrents were observed at pH 5.5 (0.053 ± 0.003 μA cm^{-2}) and pH 7.5 (0.08 ± 0.03 μA cm^{-2}). No photocurrent was observed for *c-meso*ITO|SAM-$C_2CO_2^-$ without PSII, and Mn-depleted PSII showed only a very small photocurrent of 0.027 ± 0.004 μA cm^{-2}. The Q_B site inhibitor 3-(3,4-dichlorophenyl)-1,1-dimethylurea binds to the Q_B pocket and blocks electron transfer from Q_A to Q_B. Addition of 3-(3,4-dichlorophenyl)-1,1-dimethylurea (1 mM) to the electrolyte solution for *c-meso*ITO|SAM-$C_2CO_2^-$|PSII resulted in a two-third reduction in photocurrent of DET (0.15 ± 0.01 μA cm^{-2}), suggesting a DET pathway via Q_A to the electrode in addition to the dominating electron delivery by Q_B.[6c,11,16]

The influence of SAMs with different alkyl chain lengths (SAM-$C_5CO_2^-$ and SAM-$C_{15}CO_2^-$) on photocurrent responses of *c-meso*ITO|SAM-$C_2CO_2^-$|PSII was also examined (Chart 1). Red-light-driven DET was observed with SAMs with a short alkyl chain ($C_5CO_2^-$), whereas no DET was observed with SAM-$C_{15}CO_2^-$. Addition of 2,6-dichloro-1,4-benzoquinone resulted in photocurrent via MET with all SAMs (Table 1). This result is in agreement with feasible DET and MET from PSII to ITO with a short alkyl linker, but only MET (no DET) with the insulating long alkyl chain SAM.[7b,17]

Turnover frequencies (TOFs) for PSII on *c-meso*ITO|SAM-$C_2CO_2^-$|PSII were determined to be 0.61 ± 0.12 and 4.6 ± 0.6 (mol O_2) (mol PSII)$^{-1}$ s^{-1} for DET and MET, respectively, where we assumed all PSII dimers on the electrode were photoactive (see SI). The TOF for DET with *c-meso*ITO|SAM-$C_2CO_2^-$|PSII, 0.61 ± 0.12 s^{-1}, is higher than for *e-meso*ITO|SAM-$C_2CO_2^-$|PSII (0.33 ± 0.07 s^{-1}) and *meso*ITO|PSII (0.18 ± 0.02 s^{-1}), supporting that immobilization of oriented PSII was achieved by covalent linkage after electrostatic preorientation. The photon-to-current conversion efficiency of *c-meso*ITO|SAM-$C_2CO_2^-$|PSII was determined to be ~0.01% and 0.1% for DET and MET, respectively (see SI). This result is a lower estimate, because it was assumed that the electrode absorbs all incident photons, and the quantum efficiency of PSII also increases with a lower light intensity.[6c]

In conclusion, we demonstrated covalent immobilization of preoriented PSII on a carboxylate-functionalized *meso*ITO electrode for visible light-driven water oxidation. Electrostatic interactions between PSII and the negatively charged *meso*ITO electrode orient PSII via its dipole moment in its favorable orientation for interfacial electron transfer. The carboxylates from the SAM can be covalently coupled with EDC and NHS to amine residues from amino acids in PSII. PF-PEC of PSII allowed us to determine a TOF for O_2 evolution of 0.61 ± 0.12 s^{-1} for DET using *c-meso*ITO|SAM-$C_2CO_2^-$|PSII. The reported approach gives access to biophysical studies, such as mechanistic PF-PEC of PSII, and can be extended to other photosynthetic enzymes.

■ ASSOCIATED CONTENT

Supporting Information

Experimental details, figures, and data. This material is available free of charge via the Internet at http://pubs.acs.org.

■ AUTHOR INFORMATION

Corresponding Author

reisner@ch.cam.ac.uk

Notes

The authors declare no competing financial interest.

■ ACKNOWLEDGMENTS

This work was supported by the Engineering and Physical Sciences Research Council (EP/H00338X/2), the Biotechnological and Biological Research Council (BB/K002627/1), and the Royal Society (Wolfson Merit Award).

■ REFERENCES

(1) (a) McKone, J. R.; Pieterick, A. P.; Gray, H. B.; Lewis, N. S. *J. Am. Chem. Soc.* **2013**, *135*, 223−231. (b) Reece, S. Y.; Hamel, J. A.; Sung, K.; Jarvi, T. D.; Esswein, A. J.; Pijpers, J. J. H.; Nocera, D. G. *Science* **2011**, *334*, 645−648. (c) Brillet, J.; Yum, J.-H.; Cornuz, M.; Hisatomi, T.; Solarska, R.; Augustynski, J.; Graetzel, M.; Sivula, K. *Nat. Photonics* **2012**, *6*, 824−828.

(2) (a) Ferreira, K. N.; Iverson, T. M.; Maghlaoui, K.; Barber, J.; Iwata, S. *Science* **2004**, *303*, 1831−1838. (b) Umena, Y.; Kawakami, K.; Shen, J.-R.; Kamiya, N. *Nature* **2011**, *473*, 55−60. (c) Rapatskiy, L.; Cox, N.; Savitsky, A.; Ames, W. M.; Sander, J.; Nowaczyk, M. M.; Rögner, M.; Boussac, A.; Neese, F.; Messinger, J.; Lubitz, W. *J. Am. Chem. Soc.* **2012**, *134*, 16619−16634.

(3) (a) Lubitz, W.; Reijerse, E. J.; Messinger, J. *Energy Environ. Sci.* **2008**, *1*, 15−31. (b) Ishida, N.; Sugiura, M.; Rappaport, F.; Lai, T.-L.; Rutherford, A. W.; Boussac, A. *J. Biol. Chem.* **2008**, *283*, 13330−13340. (c) Tommos, C.; Babcock, G. T. *Biochim. Biophys. Acta* **2000**, *1458*, 199−219.

(4) (a) Barroso, M.; Mesa, C. A.; Pendlebury, S. R.; Cowan, A. J.; Hisatomi, T.; Sivula, K.; Grätzel, M.; Klug, D. R.; Durrant, J. R. *Proc. Natl. Acad. Sci. U.S.A.* **2012**, *109*, 15640−15645. (b) Milano, F.; Tangorra, R. R.; Omar, O. H.; Ragni, R.; Operamolla, A.; Agostiano, A.; Farinola, G. M.; Trotta, M. *Angew. Chem., Int. Ed.* **2012**, *51*, 11019−11023. (c) Megiatto, J. D.; Antoniuk-Pablant, A.; Sherman, B. D.; Kodis, G.; Gervaldo, M.; Moore, T. A.; Moore, A. L.; Gust, D. *Proc. Natl. Acad. Sci. U.S.A.* **2012**, *109*, 15578−15583. (d) Duan, L.; Bozoglian, F.; Mandal, S.; Stewart, B.; Privalov, T.; Llobet, A.; Sun, L. *Nat. Chem.* **2012**, *4*, 418−423. (e) Subbaraman, R.; Tripkovic, D.; Chang, K.-C.; Strmcnik, D.; Paulikas, A. P.; Hirunsit, P.; Chan, M.; Greeley, J.; Stamenkovic, V.; Markovic, N. M. *Nat. Mater.* **2012**, *11*, 550−557. (f) Lin, C.-Y.; Lai, Y.-H.; Mersch, D.; Reisner, E. *Chem. Sci.* **2012**, *3*, 3482−3487. (g) Gao, Y.; Ding, X.; Liu, J.; Wang, L.; Lu, Z.; Li, L.; Sun, L. *J. Am. Chem. Soc.* **2013**, *135*, 4219−4222. (h) Tsui, E. Y.; Tran, R.; Yano, J.; Agapie, T. *Nat. Chem.* **2013**, *5*, 293−299. (i) Cheng, F.; Zhang, T.; Zhang, Y.; Du, J.; Han, X.; Chen, J. *Angew. Chem., Int. Ed.* **2013**, *52*, 2474−2477. (j) Najafpour, M. M.; Ehrenberg, T.; Wiechen, M.; Kurz, P. *Angew. Chem., Int. Ed.* **2010**, *49*, 2233−2237. (k) Wiechen, M.; Zaharieva, I.; Dau, H.; Kurz, P. *Chem. Sci.* **2012**, *3*, 2330−2339.

(5) Wang, V. C.-C.; Can, M.; Pierce, E.; Ragsdale, S. W.; Armstrong, F. A. *J. Am. Chem. Soc.* **2013**, *135*, 2198−2206.

(6) (a) Rao, K. K.; Hall, D. O.; Vlachopoulos, N.; Grätzel, M.; Evans, M. C. W.; Seibert, M. *J. Photochem. Photobiol., B* **1990**, *5*, 379−389. (b) Badura, A.; Guschin, D.; Esper, B.; Kothe, T.; Neugebauer, S.; Schuhmann, W.; Rögner, M. *Electroanalysis* **2008**, *20*, 1043−1047. (c) Kato, M.; Cardona, T.; Rutherford, A. W.; Reisner, E. *J. Am. Chem. Soc.* **2012**, *134*, 8332−8335. (d) Lee, I.; Lee, J. W.; Greenbaum, E. *Phys. Rev. Lett.* **1997**, *79*, 3294−3297. (e) Krassen, H.; Schwarze, A.; Friedrich, B.; Ataka, K.; Lenz, O.; Heberle, J. *ACS Nano* **2009**, *3*, 4055−4061. (f) Mukherjee, D.; May, M.; Vaughn, M.; Bruce, B. D.; Khomami, B. *Langmuir* **2010**, *26*, 16048−16054. (g) Manocchi, A. K.; Baker, D. R.; Pendley, S. S.; Nguyen, K.; Hurley, M. M.; Bruce, B. D.; Sumner, J. J.; Lundgren, C. A. *Langmuir* **2013**, *29*, 2412−2419. (h) Badura, A.; Esper, B.; Ataka, K.; Grunwald, C.; Wöll, C.; Kuhlmann, J.; Heberle, J.; Rögner, M. *Photochem. Photobiol.* **2006**, *82*, 1385−1390. (i) Yehezkeli, O.; Tel-Vered, R.; Wasserman, J.; Trifonov, A.; Michaeli, D.; Nechushtai, R.; Willner, I. *Nat. Commun.* **2012**, *3*, 1741/1−1741/7. (j) Yehezkeli, O.; Tel-Vered, R.; Michaeli, D.; Nechushtai, R.; Willner, I. *Small* 2013, in press (DOI: 10.1002/smll.201300051).

(7) (a) Rüdiger, O.; Abad, J. M.; Hatchikian, E. C.; Fernandez, V. M.; De Lacey, A. L. *J. Am. Chem. Soc.* **2005**, *127*, 16008−16009. (b) Ciaccafava, A.; Infossi, P.; Ilbert, M.; Guiral, M.; Lecomte, S.; Giudici-Orticoni, M. T.; Lojou, E. *Angew. Chem., Int. Ed.* **2012**, *51*, 953−956. (c) Madden, C.; Vaughn, M. D.; Díez-Pérez, I.; Brown, K. A.; King, P. W.; Gust, D.; Moore, A. L.; Moore, T. A. *J. Am. Chem. Soc.* **2012**, *134*, 1577−1582. (d) Baffert, C.; Sybirna, K.; Ezanno, P.; Lautier, T.; Hajj, V.; Meynial-Salles, I.; Soucaille, P.; Bottin, H.; Léger, C. *Anal. Chem.* **2012**, *84*, 7999−8005.

(8) (a) Pita, M.; Gutierrez-Sanchez, C.; Olea, D.; Velez, M.; Garcia-Diego, C.; Shleev, S.; Fernandez, V. M.; De Lacey, A. L. *J. Phys. Chem. C* **2011**, *115*, 13420−13428. (b) Gutiérrez-Sánchez, C.; Pita, M.; Vaz-Domínguez, C.; Shleev, S.; De Lacey, A. L. *J. Am. Chem. Soc.* **2012**, *134*, 17212−17220. (c) Blanford, C. F.; Heath, R. S.; Armstrong, F. A. *Chem. Commun.* **2007**, 1710−1712.

(9) Hoertz, P. G.; Chen, Z.; Kent, C. A.; Meyer, T. J. *Inorg. Chem.* **2010**, *49*, 8179−8181.

(10) (a) Hotchkiss, P. J.; Jones, S. C.; Paniagua, S. A.; Sharma, A.; Kippelen, B.; Armstrong, N. R.; Marder, S. R. *Acc. Chem. Res.* **2012**, *45*, 337−346. (b) Quefféléc, C.; Petit, M.; Janvier, P.; Knight, D. A.; Bujoli, B. *Chem. Rev.* **2012**, *112*, 3777−3807. (c) Muresan, N. M.; Willkomm, J.; Mersch, D.; Vaynzof, Y.; Reisner, E. *Angew. Chem., Int. Ed.* **2012**, *51*, 12749−12753.

(11) Sugiura, M.; Inoue, Y. *Plant Cell Physiol.* **1999**, *40*, 1219−1231.

(12) Loll, B.; Kern, J.; Saenger, W.; Zouni, A.; Biesiadka, J. *Nature* **2005**, *438*, 1040−1044.

(13) Felder, C. E.; Prilusky, J.; Silman, I.; Sussman, J. L. *Nucleic Acids Res.* **2007**, *35*, W512−W521.

(14) Pan, R.; Liew, K.; Xu, L.; Gao, Y.; Zhou, J.; Zhou, H. *Colloids Surf., A* **2007**, *305*, 17−21.

(15) (a) Commet, A.; Boswell, N.; Yocum, C. F.; Popelka, H. *Biochemistry* **2012**, *51*, 3808−3818. (b) Schiller, H.; Dau, H. *J. Photochem. Photobiol., B* **2000**, *55*, 138−144.

(16) (a) Larom, S.; Salama, F.; Schuster, G.; Adir, N. *Proc. Natl. Acad. Sci. U.S.A.* **2010**, *107*, 9650−9655. (b) Ulas, G.; Brudvig, G. W. *J. Am. Chem. Soc.* **2011**, *133*, 13260−13263.

(17) Khoshtariya, D. E.; Dolidze, T. D.; Shushanyan, M.; Davis, K. L.; Waldeck, D. H.; van Eldik, R. *Proc. Natl. Acad. Sci. U.S.A.* **2010**, *107*, 2757−2762.